INVESTIGATION OF AIR-COOLED CONDENSER'S OPERATING PARAMETERS IN MODERN THERMAL POWER PLANT

by

Jovan B. ŠKUNDRIĆ[a*], Predrag M. ŽIVKOVIĆ[b], Milan M. TICA[a], Mladen A. TOMIĆ[c], and Christian P. BARZ[d]

[a] Faculty of Mechanical Engineering, University of Banja Luka, Banja Luka, Republic of Srpska, B&H
[b] Faculty of Mechanical Engineering, University of Niš, Niš, Serbia
[c] Faculty of Technical Sciences, University of Novi Sad, Novi Sad, Serbia
[d] Northern University Center Baia Mare, University of Cluj-Napoca, Cluj-Napoca, Romania

Original scientific paper
https://doi.org/10.2298/TSCI220806203S

Air-cooled condensers in thermal power plants have recently become increasingly popular. Besides all the advantages they have, like no demands for water supply on the plant site and no need for taking care of environmental regulations, they also have some serious disadvantages. One of the biggest disadvantages air-cooled condensers do have is precisely the nature of the Earth's atmosphere being their low temperature reservoir. Low density and low heat capacity of the air as the cooling medium combined with extremely stochastic behavior of the atmosphere itself put some serious challenges in front of the air-cooled condenser's proper and steady functioning. In this paper, the operating parameters of the air-cooled condenser in the chosen thermal power plant were investigated to gain a clearer insight into the influence of the atmospheric changes on its entropy generation and consequently on its efficiency. Also, the acquired results were further proposed as a starting point for potential optimization of the process inside the device.

Key words: *air-cooled condenser, thermal power plant, entropy, efficiency*

Introduction

Until recently, especially in large thermal power plants, condensers were, as a rule, exclusively designed as a water-cooled. The main reason for that was the fact that degree of efficiency of the cycle by which older power plants operated was relatively low, leaving no room for additional reduction, which the use of the air-cooled condenser would certainly cause. Water-cooled condensers, obviously have some significant advantages over the air-cooled systems, primarily in terms of higher specific heat and higher density of the coolant, and, as a rule, lower coolant temperatures. But, on the other hand, they also have a significant disadvantage since, regardless of the construction, they require the existence of sufficient amount of water on-site, whether it is a river, lake, or possibly the sea. Another lack of water-cooled condensing systems refers to their negative impact to the environment especially when it comes to large plants, which was investigated by various authors, [1-4].

Air-cooled condensers become applicable in large thermal power plants only after the technology of materials used for the construction of boiler and turbine elements reached a

* Corresponding author, e-mail: jovan.skundric@gmail.com

level that allowed significant increases in fresh steam parameters, and thus allowed significant increasing of such plant's efficiency. A more detailed insight into the impact of modern materials on the plant's efficiency can be obtained through the recently published studies, [5-7]. Such modern and far more efficient plants finally leave room to implement an air-cooled steam condensing system, as their overall efficiency, even with slightly less efficient condensation, will remain within more than satisfactory limits. This further enables the building of plants at the coal mine location, even if there is not enough water on-site for the application of water-cooled condensers. Such location can still be used to construct the plant, without the additional cost for fuel or energy transport.

However, low values of air density and specific heat are not the only problem when it comes to the operation of air-cooled condensers. One of the biggest problems of such condensing systems lies in the extremely stochastic nature of the environment into which the heat from the condensing steam is dissipated. The mentioned stochastics of the environment is primarily reflected in the difficulty of wind parameters prediction, the insolation intensities during the day, as well as the deviation of ambient air temperatures from the design values. Particularly for these reasons, a number of researches have been conducted with a goal to find an optimal direction for further improvement of the air-cooled condenser design, [8-12]. Also, the complex phenomena governing the function of air-cooled condensing devices have also been the field of interest of numerous authors, [13-16].

Considering before mentioned, for a quality insight into possible operational problems of such a system, as well as to find ways to eliminate them, it is necessary to perform continuous and detailed measurements of the condenser operational parameters simultaneously with meteorological parameters on-site of the plant. One possible approach to this challenge is given in this paper on the example of thermal power plant in Stanari, Republic of Srpska.

The air-cooled condenser in thermal power plant Stanari

Thermal power plant *Stanari* is the 300 [MW] lignite-fired power plant. Since no water resources exist on the plant's site, the condenser for the plant was chosen to be the air-cooled, fig. 1. The air-cooled condenser within the plant is designed as the *A*-type external multicell device with forced draft.

The condenser itself is mounted on the steel structure, which is supported by concrete columns, and consists of modules with packages of aluminum finned steel pipes mounted on steel frames with electric motor driven axial fans that provide the flow of ambient air as a cooling medium. The condenser consists of two types of panels (packages of finned pipes) and those are primary and secondary panels. The primary, parallel-flow or direct-flow panels are designed in a way that both the steam and the condensate flow in same direction, while the secondary or counter-flow panels are designed so the steam and the condensate flow in mutually opposite directions. Part of the condenser which involves only secondary panels is also called dephlegmator.

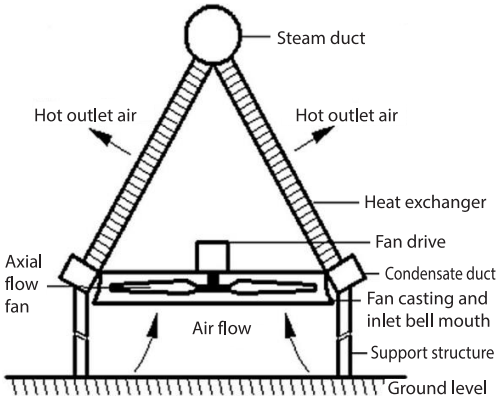

Figure 1. The *A*-type cell of air-cooled condenser

The steam discharged from the turbine is being supplied to the condenser through the duct mounted onp of the each module and

flows while condensing through the finned tubes within primary and secondary panels and finally is being collected as completely condensed in collectors positioned on the bottom of the mounting frame. Part of the duct on the top of secondary panels is connected to the group of elements for removing of non-condensable gases from the condenser. Finally, the condensate from primary and secondary sections of the condenser is further stored in the condensate tank placed beneath the low pressure turbine.

Regarding the layout and actual dimensions, the condenser consists in total of 30 cells arranged in six lanes with five cells in each lane, fig. 2. The first, the third and the fifth cell in each lane are of primary type, while the second and the fourth are of secondary (counter-flow) type. There are 300 panels in total, whereby 252 of them are of the primary type and 48 of the secondary type. Overall heat exchanging surface of the condenser is approximately 877495 m^2, while the whole condenser is 70 m long and 59 m wide.

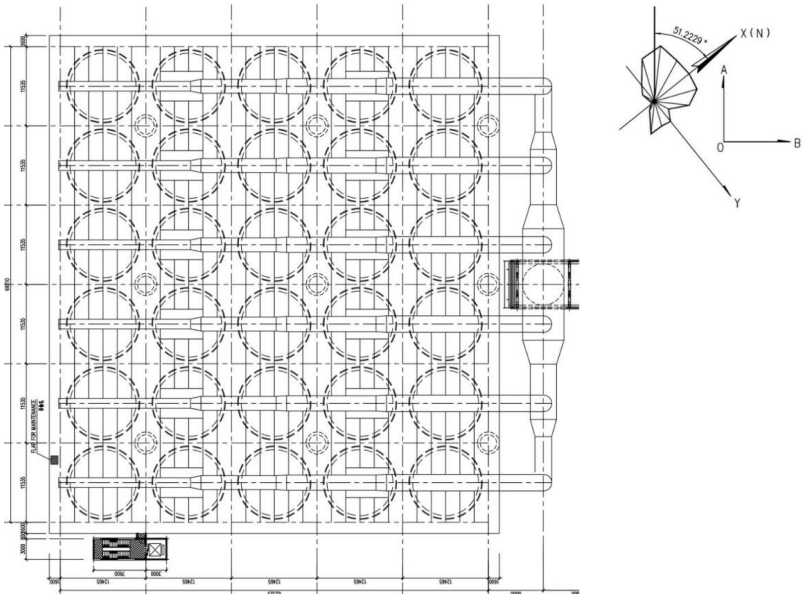

Figure 2. The air-cooled condenser disposition and orientation

Method

The main goal of the paper was to get the insight into the scale of the steam flow imbalance inside the condenser that is caused by the current meteorological conditions. The reason for this direction in investigating condenser's operating parameters was the suspicion that the side wind not only causes decreasing of convective heat transfer coefficient on certain cells due to compromised air velocity on the fan's outlet, but also causes steam flow imbalance inside the condenser. Possible imbalance would certainly cause increasing of both thermal and fluid-flow irreversibilities of the process. If so, this would mean that the side wind could also be the cause for increasing of overall generated entropy of the condenser, compromising its efficiency in the same time. For this purpose, the entropy generation minimization algorithm, given by Bejan [17] was used. By the algorithm, the generated entropy on the steam side is given:

$$\dot{S}_{\text{gen}} = \dot{Q}\frac{\Delta T}{T_0 T_{\text{in}}} + \frac{\dot{m} v_{\text{out}}}{T_{\text{in}}}\Delta p \tag{1}$$

where $\dot{Q}$ is the heat flux removed from the steam, $\dot{m}$ – the mass-flow of the steam, v_{out} – the specific volume on the condenser outlet (~ specific volume of the condensate), T_{in} – the temperature on the condenser's inlet (~ temperature of condensation), T_0 – the ambient temperature, $\Delta T = T_{in} - T_0$ – the difference between those two temperatures, and Δp – the pressure drop on the steam side.

Obviously, the first term in the eq. (1) represents the heat transfer irreversibility and the second term represents the fluid-flow irreversibility. Since the calculation was performed using the actual data and since the condenser's design is such that it pretty much is a *black box* with almost no sensors mounted on the device, the technical aspect of the analysis was a pretty challenging task. The only available readings were the process data from the power plant monitoring system which gives only parameters on the inlet and the outlet of the condenser with absolutely no information what is going on in individual cells of the condenser. Those readings were sufficient for determining T_{in} and v_{out}, but for the heat fluxes and the pressure drops in particular sections of the heat exchanging modules the proper approach still had to be found.

For that purpose, certain assumptions and simplifications of the actual physical model had been made:

– The steam was assumed to be fully condensed by the lower end of the panel (tube).
– All the panels were assumed to be of direct-flow type.
– The condensate was assumed to be in the saturated liquid state.
– The two-phase flow inside the tubes was assumed to be stratified.
– The condenser was assumed to operate in quasi steady-state.

To find the unknown magnitudes, temperatures of outer walls of the heat-exchanging surface were measured with the ScanTemp 490 Infrared thermometer, manufactured by Dostmann electronic GmbH. The ScanTemp 490 has declared accuracy of ±2% in the temperature range of –60 °C to +1000 °C. The temperatures were measured in a way to obtain readings at the mid-sections of 4 panels inside each cell (left and right panel on each side of the cell).

The steam side convective heat transfer coefficient was calculated according to Shah's improved correlation, [18]. The correlation is based on the procedure for determining one of the three given regimes the actual physical model applies to and then to calculate the convection coefficient according to the equation which obeys the actual regime. To determine the regime, two variables must be calculated:

$$J_g = \frac{xG}{\left[\mathrm{g}D_{\mathrm{int}}\rho_g\left(\rho_\ell - \rho_g\right)\right]^{0.5}} \tag{2}$$

$$Z = \left(\frac{1}{x} - 1\right)^{0.8} p_r^{\,0.4} \tag{3}$$

where J_g is the dimensionless steam velocity and Z – the so-called Shah's correlating parameter. Other variables in the eq. (2) and (3) are: x – the steam quality (mean value between the turbine exhaust state and the saturated liquid state was taken), G – the total mass flux, D_{int} – the internal diameter of the tube (the hydraulic diameter was taken), ρ_g – the density of the vapor phase and ρ_ℓ – the density of the liquid phase, p_r – the dimensionless reduced pressure. Since the calculated values for J_g and Z correspond to the Regime III, [18] the steam-side convection coefficient was further calculated according to Nusselt's equation for laminar film condensation in vertical tubes:

$$\alpha = 1.32\,\mathrm{Re}_\ell^{\,-1/3}\left[\frac{\rho_\ell\left(\rho_\ell - \rho_\mathrm{g}\right)\mathrm{g}k_\ell^{\,3}}{\mu_\mathrm{g}^{\,2}}\right]^{1/3} \tag{4}$$

where k_ℓ is the thermal conductivity of the liquid phase, μ_g – the is the dynamic viscosity of the vapor phase, while Re_ℓ is the Reynolds number for liquid phase, calculated as:

$$\mathrm{Re}_\ell = \frac{4\dot{m}(1-x)}{\pi\mu_\ell D_{\mathrm{int}}} \tag{5}$$

where $\dot{m}$ is total mass-flow of the steam and μ_ℓ – the dynamic viscosity of the liquid phase. It is also important to say that according to Shah, [18], for tubes inclined downwards at 15° or more the recommended approach is to treat them as they were vertical.

The heat fluxes were calculated according to the eq. (6) as combined convective and conductive heat transfer from the liquid film of the condensate inside the tube to the outer wall of the tube, where the temperatures were measured. Also, the resistance to the heat flow through the tube's wall was calculated according to the numerically obtained conduction shape factor:

$$\dot{Q} = \frac{Fk}{1+\dfrac{Fk}{A_{\mathrm{int}}\alpha}}\left(T_k - T_w\right) \tag{6}$$

Mass-flows of the steam were further calculated according to the known heat fluxes and the enthalpy differences for the fully condensed steam. The pressure drops on the steam side were calculated according to the equation [19]:

$$\Delta p = \lambda\rho_g \frac{w_g^2}{2d_{\mathrm{free}}} L \tag{7}$$

where λ is the friction factor on the surface of the liquid film, ρ_g – the density of the steam, w_g – the velocity of the steam, L – the length of the tube, d_{free} – and the equivalent free diameter of the tube corresponding to the free cross-section of the tube (the hydraulic diameter of the tube was taken). The velocity of the steam was calculated as the average velocity of gaseous phase with the assumption that the steam fully condenses by the end of the panel.

The friction factor on the surface of the liquid film was calculated according to the correlation, [19]:

$$\lambda = 8\left[\left(\frac{8}{\mathrm{Re}}\right)^{12} + \frac{1}{(A+B)^{1.5}}\right]^{1/12} \tag{8}$$

where A and B are constants dependent on the Reynolds number and evaluated according to [20]:

$$A = \left[2.457\ln\frac{1}{\left(\dfrac{7}{\mathrm{Re}}\right)^{0.9} + 0.27\dfrac{\varepsilon}{D}}\right]^{16} \tag{9}$$

$$B = \left(\frac{37530}{\mathrm{Re}}\right)^{16} \tag{10}$$

where ε/D in the eq. (9) is the relative roughness of the inside of the tubes.

Meteorological parameters at the plant location were measured in the meteorological station located within the plant itself, while the process data were obtained directly from the power plant monitoring system.

The given mathematical approach was later applied to the measured temperatures and obtained process data and was also applied for the hypothetical case of ideally balanced condenser's operation. For ideally balanced state of the condenser's operation the state where heat fluxes and steam mass-flows are equal for each tube was considered and was assumed to be the state with minimum entropy generation. So finally, the corresponding entropy generation numbers were calculated for each set of measured temperatures:

$$N_S = \frac{\dot{S}_{\text{gen}}}{\dot{S}_{\text{min}}} \tag{11}$$

Results and discussion

Two sets of measurements have been performed. One on a relatively calm day with an average wind speed of 1.30 m/s and another on a relatively windy day, with an average wind speed of 3.40 m/s. The results of the measurements are shown in tab. 1 and tab. 2. As in the method description part of the paper was already mentioned, the temperatures of the outer walls (inside the cells) of heat-exchanging panels front sections were measured with the IR-thermometer at 120 points, so four different measurements were performed for each cell.

Table 1. Temperatures measured at 1.30 m/s wind speed, condensing temperature 62.03 °C

°C			CELL									
			#1		#2		#3		#4		#5	
LANE	#1	*L*	56.1	56.4	56.8	56.1	57.1	57.6	57.1	59.6	57.7	57.1
		R	56.9	56.8	57.6	56.8	57.1	57.3	55.6	59.4	58.7	58.6
	#2	*L*	57.6	58.3	58.6	57.7	56.5	57.4	56.3	57.5	56.8	56.4
		R	57.9	58.1	58.8	57.9	58.2	57.2	56.7	58.5	57.6	56.8
	#3	*L*	56.7	56.8	58.3	57.5	56.8	57.7	57.0	58.7	57.6	57.8
		R	57.1	56.2	58.5	56.8	57.6	57.9	57.4	58.5	57.9	59.7
	#4	*L*	56.8	56.7	57.4	57.6	56.3	56.2	56.5	57.8	57.0	57.3
		R	56.6	55.6	58.5	57.4	57.6	56.5	56.8	58.3	57.0	57.6
	#5	*L*	55.6	55.1	57.0	57.8	57.9	57.7	56.8	58.6	56.6	57.8
		R	56.1	56.1	57.7	57.3	57.9	56.9	55.6	55.8	58.6	58.8
	#6	*L*	58.4	56.9	57.2	57.7	57.4	56.9	56.6	58.8	55.7	56.5
		R	58.1	57.4	57.3	57.9	56.6	57.7	56.3	57.4	56.5	56.6

Measurements at each cell were performed in a way that the temperatures for left and right section on each side of the cell were measured. Each of those sections includes approximately 76.5 tubes according to the specified dimensions of the cells and the specified dimensions of each tube given by the manufacturer's specification. It should be noted that for certain cells from the second data set, some of the measured temperatures appeared to be slightly higher than the actual condensation temperature. Those values were considered equal to the actual condensation temperature and the differences in readings were attributed to the declared error of the IR-thermometer. It was also assumed that cells where the measured temperatures were equal to the condensation temperature were out of the function at the time and that no heat flux was being distributed through those heat exchanging surface sections.

Table 2. Temperatures measured at 3.40 m/s wind speed, condensing temperature 59.76 °C

°C			CELL									
			#1		#2		#3		#4		#5	
LANE	#1	*L*	49.5	50.1	50.1	51	50.6	51.4	52.1	54.1	52.7	52.8
		R	52.6	51.6	49.6	51.4	51.6	51.6	49.8	53.8	52	55.8
	#2	*L*	52.6	53.4	54.4	52.1	54.4	53.4	53.8	53.8	56.4	56.1
		R	52.7	52.4	52.6	52.9	55.9	54.1	54.6	54.5	55.5	55.1
	#3	*L*	54.9	55.1	56	55.1	55	55	55.1	55.7	55.8	55.9
		R	53.1	53	55.7	55.4	55.1	55.2	55.7	55.1	55.4	55.8
	#4	*L*	55	54.4	55.7	55.6	56.1	56	56.7	58.3	58.3	61
		R	53.9	54.2	54.8	54.1	55.1	55.2	55.1	55.4	58.3	60.5
	#5	*L*	57.1	56.7	57.1	54.6	56.8	56.1	55.8	57.5	58.7	60.1
		R	58.9	56.9	56.8	54.2	56.4	54.9	56.9	59.4	59.6	58.5
	#6	*L*	57.4	59.8	60.4	55.4	55.4	55.5	55.4	60.7	57.9	60.3
		R	58.3	59.6	59.1	59	57.9	56.8	56.4	56.8	60.4	59.5

For the first set of measurements, the overall heat flux calculated according to the measured temperatures differed from the heat flux calculated according to the process data (readings from the power plant's monitoring system) by 3.7% while for the other set of measurements the difference was 5.2%. The same deviation from the process data was also present in calculated steam mass-flows. These differences originate in the method the convection coefficients were calculated. The convection coefficients were calculated for both sets of the data for an ideally balanced condenser (equal mass-flows through each panel calculated according to the process data), which means that the rest of the calculation was performed according to the average values of the coefficient. Since the actual operating states at the time of the measurements were certainly not ideally balanced, the scale of the imbalance directly influenced the deviation of local convection coefficients from the average value, increasing the overall deviation of the results.

On the figs. 3-10 the calculated data are presented. For easier presentation, at the diagram's horizontal axis, Numbers 1 and 2 refer to the first cell, Numbers 3 and 4 to the second and so on. Each point on diagrams refers to a package of 76.5 tubes or one quarter of one cell.

At the first glance, the considerably higher dissipation of the results can be seen on diagrams that refer to the second data set. As expected, the operating condition of the condenser during the windier day was much more out of the balance than the calm day operating condition, which also explains the higher obtained error for that set of the data. The dash-dotted line on each diagram refers to the average value of the calculated results. The average values of the heat flux and the mass-flow of the steam refer to the ideally balanced condenser for the actual condensation pressure for each data set.

One cannotice that the obtained friction coefficients were in a good compliance with the available data, for the average Reynolds number values within $3.65 \cdot 10^4$ to $3.84 \cdot 10^4$ and the relative roughness of the tube of $1.48 \cdot 10^{-3}$ for the flow over the liquid film. For the first data set, friction coefficient was in average $2.69 \cdot 10^{-2}$ with standard deviation of $3.502 \cdot 10^{-3}$ and for the other set $2.23 \cdot 10^2$ in average with standard deviation of $1.335 \cdot 10^{-2}$. The calculated pressure drops were in average 232.5 Pa for the first data set and 350.7 Pa for the second and both cal-

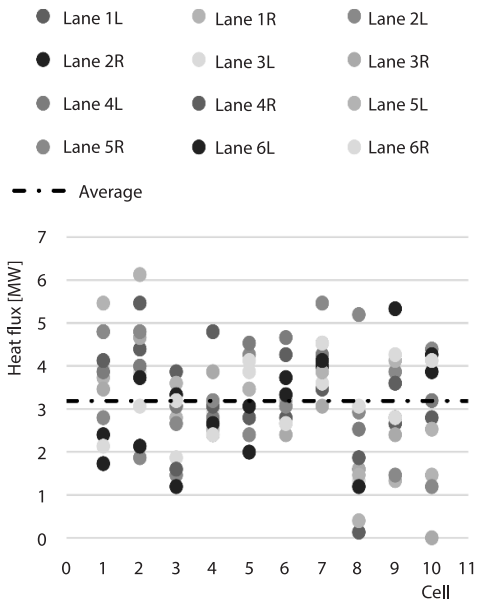

Figure 3. Heat flux for 1.30 m/s wind speed

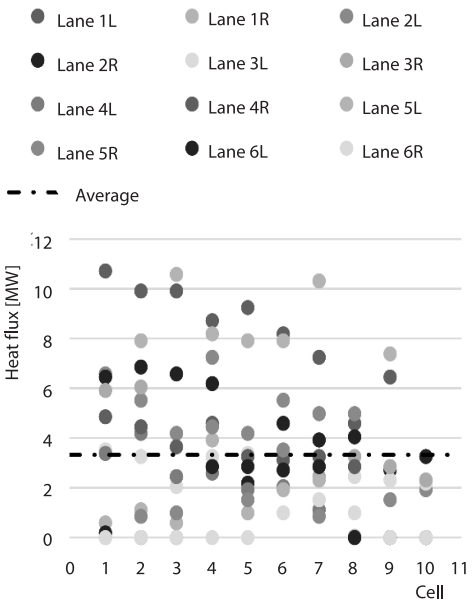

Figure 4. Heat flux for 3.40 m/s wind speed

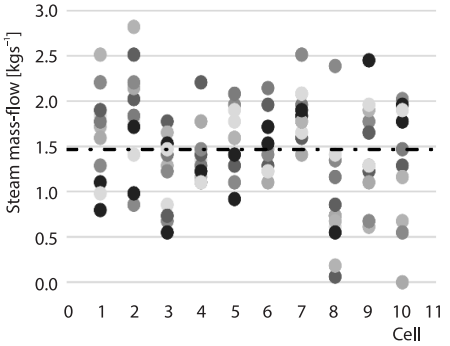

Figure 5. Mass-flow for 1.30 m/s wind speed

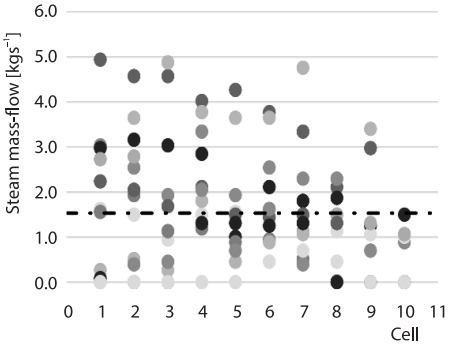

Figure 6. Mass-flow for 3.40 m/s wind speed

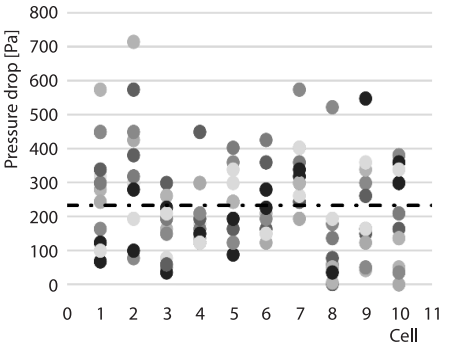

Figure 7. Pressure drop for 1.30 m/s wind speed

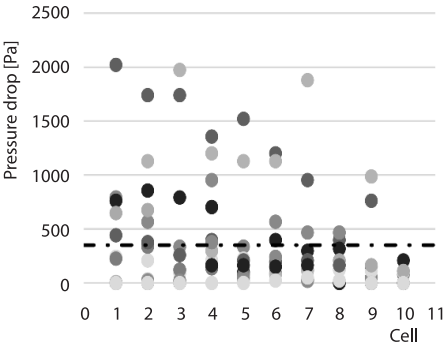

Figure 8. Pressure drop for 3.40 m/s wind speed

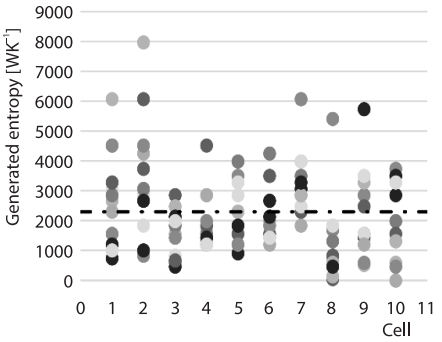

Figure 9. Generated entropy for 1.30 m/s wind

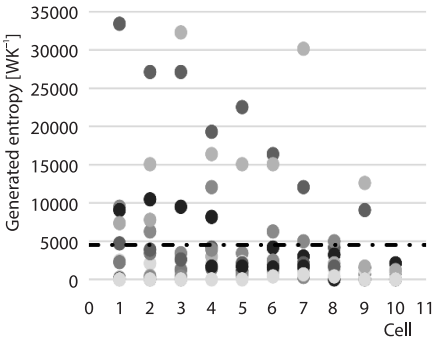

Figure 10. Generated entropy for 3.40 m/s wind

culated values were in reasonably good compliance with the pressure drop that corresponds to the temperature differences between condenser's inlet and the outlet.

Finally, the average entropy generated per cell for the first measurement set was 2300 W/K with standard deviation of 1483 W/K and for the other set was 4504 W/K with standard deviation of 7047 W/K. At the same time, the generated entropies which correspond to the ideally balanced operating states were 1970 W/K and 2038 W/K, respectively.

This shows that average corresponding entropy generation numbers were 1.17 for the first data set and 2.21 for the other. Also, the overall generated entropies, calculated according to the average pressure drops were $2.53 \cdot 10^5$ W/K and $3.27 \cdot 10^5$ W/K, respectively for the first and for the second data set, while the corresponding generated entropies for the ideal cases were $2.36 \cdot 10^5$ W/K and $2.45 \cdot 10^5$ W/K, respectively. So, the overall entropy generation numbers were 1.07 for the first set and 1.34 for the other.

By observing the generated entropies presented on the figs. 9 and 10 the very interesting occurrence can be noticed. If we consider panels which generate more entropy than 3000 W/K as those with high entropy generation, and panels which generate less entropy than 1000 W/K as those with low entropy generation. As presented, exactly the panels with low generated entropies are also the ones with the lowest mass-flows and with the lowest distributed heat fluxes while the ones with the highest generated entropies seem to perform most of the process. Obviously, the problematic panels are not the ones which generate entropy above the average but exactly the ones with entropy generation below the average and especially the ones with generated entropy close to zero. Moreover, it seems that sub-functioning panels with consequently below average entropy generation cause overloading of the rest of the panels increasing their irreversibility and disrupting the overall condenser efficiency.

Conclusion

It is presented that the most challenging part of the air-cooled condenser performance and application in modern thermal power plants is exactly the Earth's atmosphere being the low temperature reservoir for the process. Sudden and often hard to predict changes in the atmosphere could lead to serious disruptions of the air-cooled plant functioning. The most dramatic scenario arises during hot summer days when the condenser operates on the top nominal parameters of the atmosphere. During those periods even a slight additional disturbance can cause severe operating problems. Those disturbances can be caused either by additional temperature rise or by the sudden gust of the side wind or, for the worst-case scenario, by both.

In such cases, obviously an additional boost of condensing potential must be engaged in order to preserve the projected cooling capacity of the condenser. One of the possible solutions is a hybrid system which uses water-spray injected in the air-flow to increase the cooling potential of the system. The additional cooling water increases the operating costs and should be used in limited quantities and economically. The mathematical approach given in this paper could help in optimizing the quantities of the cooling water in a way to engage the hybrid system only for cells with the lowest entropy generation. Doing so, increasing the overall heat flux and improvement of the condenser's efficiency could be simultaneously achieved by keeping the condenser reasonably balanced.

Nomenclature

A_{int} – internal surface area of tube, [m^2]
D – diameter of tube, [m]
d_{free} – equivalent free diameter of tube [m]
F – conduction shape factor of tube, [m]
G – mass flux, [kgm^{-2}s^{-1}]
g – gravitational acceleration, [ms^{-2}]
J_g – dimensionless steam velocity, [–]
k – thermal conductivity, [Wm^{-1}K^{-1}]
L – length of tube [m]
$\dot{m}$ – mass-flow, [kgs^{-1}]
N_S – entropy generation number, [–]
p – pressure, [Pa]
p_r – reduced pressure, [–]
$\dot{Q}$ – heat flux, [W]
Re – Reynolds number, [–]
$\dot{S}$ – generated entropy, [WK^{-1}]
T – temperature, [K]
v – specific volume, [m^{3}kg^{-1}]
w – velocity of steam, [ms^{-1}]
x – quality of steam, [–]
Z – Shah's correlating parameter, [–]

Greek symbols

α – convective heat transfer coeff., [Wm^{-2}K^{-1}]
ε – absolute roughness of tube, [mm]
λ – Darcy friction factor, [–]
μ – dynamic viscosity, [Pas]
ρ – density, [kgm^{-3}]

Subscripts

gen – generated
0 – environment, low temperature reservoir
in – inlet
out – outlet
int – internal
g – gaseous phase
ℓ – liquid phase
min – minimum

References

[1] Nazar, R., Water-Reduction Potential of Air-Cooled Condensers in Coal Power Plants in India and Anticipated Trade-Offs, *Applied Water Scienc*e, *10* (2020), June, 162
[2] Jočevski, M., *et al*., Thermal Pollution of a Thermal Power Plant with Once-through Cooling Systems: A Numerical Study, *Innovative Mechanical Engineering*, *1* (2022), 1, pp. 128-138
[3] Glazyrin, S. A., *et al*., Study of the Possibilities of Integrated Treatment of Flue Gases and Waste-Water from Coal-Fired Heat po Plants, *Thermal Science*, *25* (2021), 6A, pp. 4333-4345
[4] Schulze, C., Raabe, B., Herrmann, C., Thiede, S., Environmental Impacts of Cooling Tower Operations – The Influence of Regional Conditions on Energy and Water Demands, *Proceedings*, 25th CIRP Life Cycle Engineering (LCE) Conference, Copenhagen, Denmark, 2018, pp. 277-282
[5] Simić, M., *et al*., High Temperature Materials: Properties, Demands and Applications, *Hem. Ind*., *74* (2020), 4, pp. 273-284
[6] Golubovic, T., *et al*., Welded Joints as Critical Regions in Pressure Vessels Case Study of Vinyl Chloride Monomer Storage Tank, *Hem. Ind*., *72* (2018), 4, pp. 177-182
[7] Pavkov, V., *et al*., Eksperimentalno i umeričko ispitivanje cevnog luka urađenog od cevi izlaznog međupregrejača pare nakon eksploatacije (in Serbian), *Hem. Ind*., *74* (2020), 1, pp. 51-63
[8] Klimes, L., *et al*., Semi-Empirical Balance-Based Computational Model of Air-Cooled Condensers with the A-Frame Lay-Out, *Energy*, *182* (2019), Sept., pp. 1013-1027
[9] Plessis, J., Owen, M., A Single-Stage Hybrid (Dry/Wet) Dephlegmator for Application in Air-Cooled Steam Condensers: Performance Analysis and Implications, *Thermal Science and Engineering Progress*, *26* (2021), Dec., 101108
[10] Starace, G., *et al*., Experimental Performance Comparison between Circular and Elliptical Tubes in Evaporative Condensers, *Journal of Thermal Analysis and Calorimetry*, *147* (2022), July, pp. 6363-6373

[11] Camaraza-Medina, Y., *et al*., Simplified Analysis of Heat Transfer through a Finned Tube Bundle in Air Cooled Condenser-Second Assessment, *Mathematical Modelling of Engineering Problems*, *5* (2018), 4, pp. 365-372
[12] Owen, M., Kroger, D., The Effect of Screens on Air-Cooled Steam Condenser Performance under Windy Conditions, *Applied Thermal Engineering*, *30* (2010), 16, pp. 2610-2615
[13] Zhang, Z., *et al*., A Numerical Study on Condensation Heat Transfer and Pressure Drop Characteristics of Low Pressure Vapor in a Plate Heat Exchanger, *Thermal Science*, *25* (2021), 1B, pp. 665-677
[14] Abed, A., *et al*., Comparative Study on Steady and Unsteady Heat Transfer Analysis of a Spherical Element Using Air/Water Mist Two-Phase Flow, *Thermal Science*, *25* (2021), 1B, pp. 625-635
[15] Naghibi, F., *et al*., Comparison of Well-Posedness Criteria of Two-Fluid Models for Numerical Simulation of Gas-Liquid Two-Phase Flows in Vertical Pipes, *Thermal Science*, *26* (2022), 2B, pp. 1245-1265
[16] Zhou, N., *et al*., Heat Transfer Performance and Influences of Spray Cooling under Quenching, *Thermal Science*, *25* (2021), 6B, pp. 4805-4815
[17] Bejan, A., Entropy Generation Minimization, in: *The Method of Thermodynamic Optimization of Finite-Size Systems and Finite-Time Processes*, CRC Press, New York, USA, 1996
[18] Shah, M. M., An Improved and Extended General Correlation for Heat Transfer During Condensation in Plain Tubes, *HVAC R Res*, *15* (2009), 5, pp. 889-913
[19] Munson, B. R., *et al*., *Fundamentals of Fluid Mechanic*s, 7th ed., Wiley, New York, USA, 2012
[20] Churchill, S. W., Friction-Factor Equation Spans all Fluid-Flow Regimes, *Chem. Eng*., *84* (1977), 24, pp. 91-92

Paper submitted: August 6, 2022
Paper revised: October 28, 2022
Paper accepted: October 31, 2022